Activity-regulated Somatostatin Expression Reduces Dendritic Spine Density and Lowers Excitatory Synaptic Transmission via Postsynaptic Somatostatin Receptor 4[*]

Zai-Hua Hou[‡§] and Xiang Yu[‡1]

From the [‡]Institute of Neuroscience and State Key Laboratory of Neuroscience, Shanghai Institutes for Biological Sciences, Chinese Academy of Sciences, Shanghai 200031, China and the [§]University of Chinese Academy of Sciences, Shanghai 200031, China

Background: Little is known about the function of activity-induced factors secreted by interneurons.
Results: Activity-induced somatostatin expression and secretion reduced dendritic spine density and lowered excitatory synaptic transmission via somatostatin receptor 4 signaling.
Conclusion: Somatostatin reduced the density of morphological and functional excitatory synapses.
Significance: Somatostatin, an interneuron-derived secreted factor, can function to prevent epileptiform activity by reducing the number of excitatory synapses.

Neuronal activity regulates multiple aspects of the morphological and functional development of neural circuits. One mechanism by which it achieves this is through regulation of gene expression. In a screen for activity-induced genes, we identified somatostatin (SST), a neuropeptide secreted by the SST subtype of interneurons. Using real time quantitative PCR and ELISA, we showed that persistent elevation of neuronal activity increased both the gene expression and protein secretion of SST over a relatively prolonged time course of 48 h. Using primary hippocampal neuronal cultures, we found that SST treatment for 1 day significantly reduced the density of dendritic spines, the morphological bases of excitatory synapses. Furthermore, the density of pre- and postsynaptic markers of excitatory synapses was significantly lowered following SST treatment, whereas that of inhibitory synapses was not affected. Consistently, SST treatment reduced the frequency of miniature excitatory postsynaptic currents, without affecting inhibition. Finally, lowering the endogenous level of SST receptor subtype 4 in individual hippocampal pyramidal neurons significantly blocked the effect of SST in reducing spine density and excitatory synaptic transmission in a cell autonomous fashion, suggesting that the effect of SST in regulating excitatory synaptic transmission is mainly mediated by SST receptor subtype 4. Together, our results demonstrated that activity-dependent release of SST reduced the density of dendritic spines and the number of excitatory synapses through postsynaptic activation of SST receptor subtype 4 in pyramidal neurons. To our knowledge, this is the first demonstration of the long term effect of SST on neuronal morphology.

Neuronal activity is critical to the normal development of neural circuits (1–6). Of the wide array of mechanisms by which neuronal activity regulates neural circuit development, an important one is through regulating the expression of small secreted molecules, which have the potential and capability of affecting a large number of cells. Activity-induced expression of secreted molecules, such as BDNF and neuronal activity-regulated pentraxin (Narp), have been shown to modulate many aspects of neuronal function, including the development of axonal and dendritic arbors, morphological changes of dendritic spines, the formation of synapses, and plasticity of synaptic transmission (7–9). Compared with our knowledge of the function of secreted factors from projecting glutamatergic neurons such as hippocampal pyramidal neurons, relatively little is known about the effect of activity-induced factors secreted by interneurons. However, because interneurons are much fewer in number compared with projecting neurons, one would imagine that secretion of diffusible factors by interneurons could be an important mechanism by which they communicate with the large number of neighboring projecting neurons.

In a microarray screen for activity-induced genes using primary hippocampal neuronal cultures, we identified somatostatin (SST),[2] a neuropeptide synthesized and secreted by the SST subtype of interneurons, which represent ~30% of total interneurons in the neocortex and hippocampus (10–12). This result was consistent with previous studies implicating a role for SST in epilepsy (13, 14). Although SST was not the secreted molecule with the highest fold change in our microarray analysis, its broad expression in hippocampal and cortical interneurons drew our attention to its likely function during activity-dependent development. SST, first discovered in 1973 (15), is present in two bioactive forms, SST-14 and SST-28, with SST-14 being the predominant form in the brain (16). SST interneurons are dendrite-targeting interneurons displaying

---

[1] To whom correspondence should be addressed: Inst. of Neuroscience, 320 Yue Yang Rd., Shanghai 200031, China. Tel.: 86-21-54921827; E-mail: yuxiang@ion.ac.cn.

[2] The abbreviations used are: SST, somatostatin; mEPSC, miniature excitatory postsynaptic current; mIPSC, miniature inhibitory postsynaptic current; DIV, day(s) in vitro; KA, kainic acid; TTX, tetrodotoxin; qPCR, quantitative PCR; MAP, microtubule-associated protein; SSTR4, SST receptor subtype 4; GluR2, AMPA-selective glutamate receptor 2; vGluT1, vesicular glutamate transporter 1; vGAT, vesicular GABA transporter; GABA$_A$Rα1, GABA$_A$ receptor subtype α1; GAD67, glutamate decarboxylase 67.

low spike threshold and spike rate adaptation (11, 17, 18). An important subgroup, known as Martinotti cells in the neocortex and oriens-lacunosum molecular neurons in the hippocampus, modulates the excitability of pyramidal cells by negatively regulating the summation of synaptic inputs in apical dendrites (19–22). Martinotti cells also mediate disynaptic inhibition between pyramidal cells and recurrent feedback inhibition onto presynaptic pyramidal neurons, thereby preventing excessive and recurrent excitation in neuronal circuits (22–24).

Consistent with the function of SST-positive interneurons in reducing the excitability of targeting pyramidal neurons, SST is generally considered an inhibitory factor that can be secreted from axonal terminals through dense core vesicles (13) or through local dendritic release (25). Acute application of SST to hippocampal slices has been shown to increase two types of potassium currents: the voltage-sensitive M-current (26, 27) and a voltage-insensitive leak current (28), resulting in hyperpolarization of the neurons. Acute application of SST to hippocampal cultures and slices also reduced excitatory transmission via presynaptic block of glutamate release (29, 30). These reported effects of SST on reducing neuronal excitability and excitatory synaptic transmission are consistent with its anti-epileptic effect (14, 31). However, most of the previously described effects of SST are fast acting and relatively short lived, in that they were reversed upon washout. Whether SST also had longer lasting effects is relatively unknown.

In this study, we found that treating primary hippocampal neuronal cultures with SST for the relatively extended period of 24 h significantly reduced the density of dendritic spines, the morphological bases of excitatory synapses in glutamatergic projecting neurons. Furthermore, the frequency of miniature excitatory postsynaptic currents (mEPSCs) was also significantly reduced following SST treatment, whereas that of miniature inhibitory postsynaptic currents (mIPSCs) was not affected. Consistently, the number of excitatory synapses, as measured by the density of the postsynaptic marker AMPA-selective glutamte receptor 2 (GluR2), and that of the presynaptic marker vesicular glutamate transporter 1 (vGluT1) were significantly lowered following 24 h of SST treatment, whereas those of the inhibitory synaptic markers, vesicular GABA transporter (vGAT) and $GABA_A$ receptor $\alpha1$ ($GABA_AR\alpha1$), were not altered. Furthermore, knocking down the endogenous level of SST receptor subtype 4 (SSTR4) in pyramidal neurons abolished the effect of SST in reducing dendritic spine density and mEPSC frequency. In summary, we found that SST, secreted by the SST subtype of interneurons, can reduce the density of dendritic spines and lower the number of excitatory synapses in hippocampal pyramidal neurons, via postsynaptic SSTR4 activation.

EXPERIMENTAL PROCEDURES

Hippocampal Neuronal Cultures and Transfection—High density mixed neuronal-glial cultures were prepared from postnatal day 0 Sprague-Dawley rat pups as previously described (32, 33) and according to procedures approved by the Institutional Animal Care and Use Committee of the Institute of Neuroscience of the Chinese Academy of Sciences (Shanghai, China). The dentate gyrus was removed during the dissection, leaving CA1 and CA3 pyramidal neurons as the main glutama-

tergic neuronal types in the preparation. For electrophysiological recordings and immunocytochemistry, neurons were transfected with GFP using the calcium phosphate method at days *in vitro* (DIV) 8 and assayed at DIV 11–13. For spine density analysis, the neurons were transfected with the fluorescent protein tdTomato (34) (gift of Dr. Zilong Qiu, Institute of Neuroscience) using the calcium phosphate method at DIV 8–10 and fixed at DIV 15 and 16. The low transfection efficiency of this method ensures that the fluorescently labeled, transfected neuron is surrounded by untransfected presynaptic contacts.

DNA Constructs and Pharmacological Treatment—The SSTR4 RNAi sequence, cloned into pSuper vector, was targeted against the sequence GCAGCTTCTGAATCTGTTT. Specifically, the complementary oligonucleotides GATCCCC-GCAGCTTCTGAATCTGTTTttcaagagaAAACAGATTCA-GAAGCTGCTTTTTGGAAA and AGCTTTTCCAA-AAAGCAGCTTCTGAATCTGTTTtctcttgaaAAACAGAT-TCAGAAGCTGCGGG were synthesized, annealed into double-stranded DNA, and inserted into the HindIII and BglII restriction sites of pSuper.

Pharmacological treatments included 20 μM bicuculline (Tocris), 10 μM kainic acid (KA; Tocris), 10 mM KCl (Sigma), 0.5 μM tetrodotoxin (TTX; Fisheries Science and Technology Development), and 1 μM SST (Sigma). Cultured neurons were treated with pharmacological reagents for 4–48 h as indicated. For *in vivo* KA injections, postnatal day 14 rats or 2-month-old glutamate decarboxylase 67 (GAD67)-GFP heterozygous mice (gift of Dr. Yuchio Yanagawa, Kyoto University) (35) were intraperitoneally injected with KA at 3.5 or 15 μg/g, respectively, and sacrificed 6 or 24 h later.

Microarray Analysis, Real Time Quantitative PCR (qPCR), and ELISA—Primary hippocampal neuronal cultures were treated with bicuculline and/or TTX for 4 or 48 h as indicated. On DIV 12, total RNA was extracted using the TRIzol reagent (Invitrogen). Microarray analysis was performed using Agilent whole rat genome microarray (G4131F-014879) by Shanghai Biotechnology Corporation (Shanghai, China), according to the manufacturer's protocols. Three independent culture preparations were assayed, and the results, measured as fold change relative to untreated control of each batch, were averaged.

For brain mRNA isolation, rats were deeply anesthetized with intraperitoneal injection of 0.7% sodium pentobarbital. Hippocampi were dissected, and total RNA was extracted using the TRIzol reagent (Invitrogen) following the manufacturer's instructions.

For real time qPCR experiments, mRNA was reverse transcribed by oligo(dT) priming using SuperScriptIII reverse transcriptase (Invitrogen), following the manufacturer's protocols. The primers used for qPCR were: SST (forward, GCCAC-CGGGAAACAGGAACTGG; reverse GGGTGCCATGGC-TGGGTTCG); and GAPDH (forward, CTGCCCAGAACAT-CATCCCT; reverse, TGAAGTCGCAGGAGACAACC). Real time qPCRs were performed using SYBR Green Master Mix (TaKaRa) on an ABI PRISM 7000 sequence detection system (Applied Biosystems). All of the reactions were performed in triplicates, and the relative amount of SST mRNA (normalized to GAPDH) was calculated using the comparative C_T method (36). To assay the level of secreted SST, the medium of cultured

neurons was harvested and assayed using an SST ELISA kit (EK-060-03; Phoenix Pharmaceuticals, Inc.) following the manufacturer's instructions.

Immunostaining, Image Acquisition, and Analysis—Immunocytochemistry for hippocampal neuronal cultures was carried out as previously described (32). For surface GluR2 staining, GluR2 antibody (mouse, 1:200, Millipore) was added to the medium of cultured neurons for 15 min at 37 °C prior to fixation. Other primary antibodies included: microtubule-associated protein 2 (MAP2, chick, Millipore, 1:1000), MAP2 (mouse, Sigma, 1:500), SST (goat, Santa Cruz, 1:500), GABA (rabbit, Sigma, 1:1500), Bassoon (guinea pig, Synaptic Systems, 1:500), Bassoon (mouse, Stressgen, 1:500), vGluT1 (guinea pig, Millipore, 1:500), vGAT (rabbit, Synaptic Systems, 1:500), and $GABA_A R\alpha 1$ (rabbit, Alomone Labs, 1:200).

Immunohistochemistry in brain slices was carried out using GAD67-GFP heterozygous mice (35), according to standard protocols as previously described (37). The following primary antibodies were used: SST (goat, Santa Cruz, 1:200) and GFP (rabbit, Invitrogen, 1:500). The nuclei were labeled using TO-PRO-3 (1:2500, Invitrogen). Alexa Fluor 488, 568, or 633 secondary antibodies (Invitrogen) were used at 1:1000 for neuronal cultures and at 1:500 for brain slices.

Images (Z-stacks) were acquired on a Zeiss LSM Pascal laser scanning confocal microscope (Jena, Germany) using a 20× Plan-Apochromat objective (N.A. = 0.8) at 1× optical zoom for SST immunostaining in culture and brain slices and a 63× oil immersion Plan-Apochromat objective (N.A. = 1.4) at 2× optical zoom for synaptic puncta analyses. Analysis of synaptic puncta was carried out as previously described (32) using custom macros. Puncta density refers to the number of puncta per micrometer of dendrite, whereas integrated intensity refers to the average intensity of puncta in the selected dendritic segment (GFP fluorescence or MAP2 immunostaining). For analysis of spine density and size, the spines were manually counted, and the lengths of dendrites and the sizes of spines were measured with ImageProPlus software (MediaCybernetics). All of the images were analyzed blindly.

Electrophysiological Recordings in Cultured Neurons—Whole cell patch clamp recordings were carried out at room temperature on DIV 11–13 neurons using a Multiclamp 700B amplifier (Molecular Devices) as previously described (32). The extracellular solution contained 129 mM NaCl, 5 mM KCl, 30 mM glucose, 25 mM HEPES, 2 mM $CaCl_2$, 1 mM $MgCl_2$ (pH 7.3, 310 mOsm). For mEPSC recordings, 0.5 μM TTX and 50 μM picrotoxin (Tocris) were added to the extracellular solution; for mIPSC recordings, 0.5 μM TTX and 5 μM NBQX (Tocris) were added. Analysis of mPSCs was performed blindly using the Mini Analysis Program (Synaptosoft) with an amplitude threshold of 3 pA for mEPSCs or 5 pA for mIPSCs. Cumulative distributions were generated using 150 consecutive mPSCs, averaged across all cells.

Western Blot Analysis—For assaying the efficiency of SSTR4 RNAi, the RNAi plasmid was transfected into neuronal cultures using electroporation. On DIV 6, neurons were harvested with radioimmunoprecipitation assay lysis buffer containing protease inhibitor mixture tablets (Roche Applied Science). Western blot was performed and quantified as previously described (38).

Primary antibodies included: GAPDH (1:10,000, Kangchen Bio-tech) and SSTR4 (1:1500, Santa Cruz Biotechnology).

Statistical Analysis—For all imaging and electrophysiology experiments, statistical analyses were carried out using two-tailed unpaired Student's t test (for sample pairs) or one-way analysis of variance (for three or more conditions). Cumulative distributions were compared using the Kolmogorov-Smirnov two-sample test. At least three independent culture preparations were used per experiment. The results are shown as the means ± S.E., and n represents the number of neurons for electrophysiological and morphological analyses. For real time qPCR and ELISA, n represents the number of independent culture preparations or the number of animals. All of the results statistically different from control are marked. *, $p < 0.05$; **, $p < 0.01$; ***, $p < 0.001$.

RESULTS

The Expression and Secretion of SST Were Increased Following Increased Neuronal Activity—In a screen for activity-induced genes in DIV 12 primary hippocampal neuronal cultures, we identified SST, a neuropeptide synthesized by ~30% of cortical and hippocampal interneurons (10–12). Global elevation of neuronal activity using the $GABA_A$ receptor antagonist bicuculline (20 μM) significantly increased SST expression at both the 4- and 48-h time points (Fig. 1A). Importantly, the elevation in SST expression was specific to activity changes, because co-incubation with the sodium channel antagonist TTX (blocks action potentials, 0.5 μM) abolished the effect of bicuculline treatment on inducing SST mRNA expression (Fig. 1A). These results were further confirmed by global application of various pharmacological reagents that elevate neuronal activity via distinct mechanisms, including bicuculline (20 μM) to block $GABA_A$ receptor-mediated inhibition, KA (10 μM) to increase excitatory synaptic transmission through activation of the AMPA and kainate subtypes of ionotropic glutamate receptors, and depolarizing neurons with elevated extracellular potassium (10 mM KCl). Real time qPCR results showed that the mRNA level of SST was significantly elevated following all three manipulations at both the 4- and 48-h time points (Fig. 1B), further demonstrating that the expression of SST was activity-dependent. To examine whether neuronal activity also regulated the expression of SST *in vivo*, postnatal day 14 rats were intraperitoneally injected with KA (3.5 μg/g) and sacrificed for analyses 6 or 24 h later. Consistent with our results from cultured neurons, the hippocampal mRNA level of SST was significantly increased 6 and 24 h following KA injection (Fig. 1C), demonstrating that elevated neuronal activity can induce SST expression *in vivo*. Because SST is a secreted neuropeptide, we next asked whether neuronal activity also regulated the secretion of SST. Harvesting the medium of neuronal cultures at 4, 12, 24, and 48 h following initiation of bicuculline treatment, we found that the level of SST in the medium was significantly increased at the 24- and 48-h time points, as assayed by ELISA (Fig. 1D). Thus, neuronal activity induced SST secretion, but with a slower time course than changes in its gene expression. Taken together, these results showed that global and persistent elevation of neuronal activity increased SST expression both *in vitro* and *in vivo* and also enhanced its secretion.
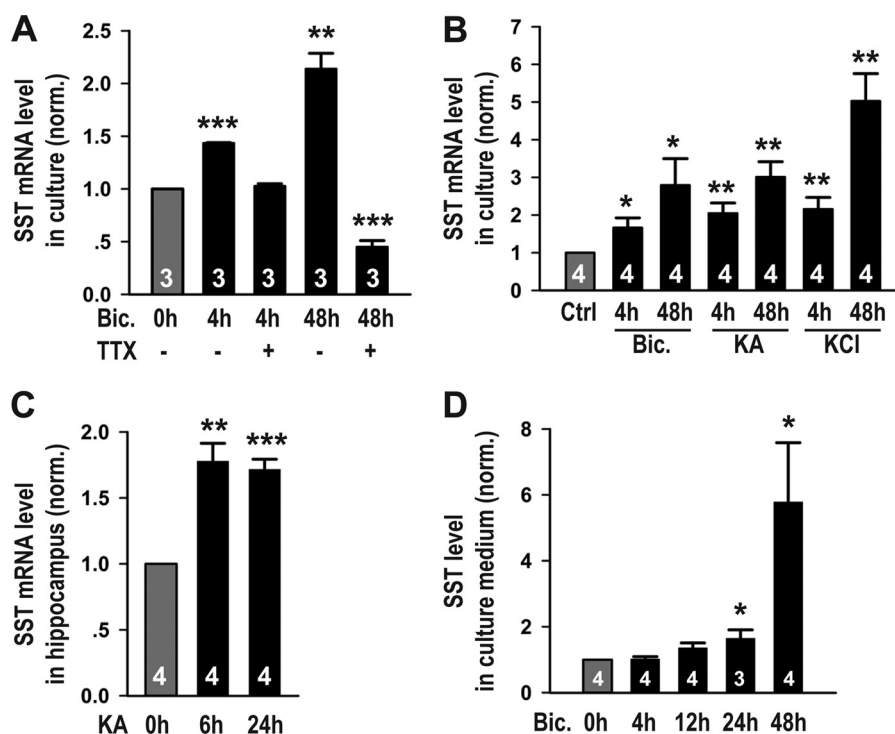
FIGURE 1. **Neuronal activity increased the expression and secretion of SST.** *A*, microarray results from three independent hippocampal neuronal culture preparations showed that SST mRNA level was significantly elevated following global activity elevation with bicuculline (*Bic.*) and blocked by co-application of TTX (*Bic.*, 4 h: 1.43 ± 0.005, $p < 0.001$; *Bic.*, 4 h + TTX: 1.03 ± 0.02, $p > 0.05$; *Bic.*, 48 h: 2.14 ± 0.15, $p < 0.01$; *Bic.*, 48 h + TTX: 0.45 ± 0.06, $p < 0.001$). *B*, real time qPCR results from additional culture preparations showing that the SST mRNA level was significantly increased following different manipulations that elevated neuronal activity for 4 or 48 h (*Bic.*, 4 h: 1.66 ± 0.26, $p < 0.05$; *Bic.*, 48 h: 2.79 ± 0.71, $p < 0.05$; KA 4 h: 2.05 ± 0.27, $p < 0.01$; KA 48 h: 3.01 ± 0.41, $p < 0.01$; KCl 4 h: 2.16 ± 0.31, $p < 0.01$; KCl 48 h: 5.03 ± 0.73, $p < 0.01$). *C*, real time qPCR results showed that SST expression in the hippocampus was up-regulated following KA injection *in vivo* (KA 6 h: 1.78 ± 0.14, $p < 0.01$; KA 24 h: 1.72 ± 0.08, $p < 0.001$). *D*, ELISA results showed that the level of SST in the medium of hippocampal neuronal cultures was elevated following bicuculline treatment (4 h: 1.02 ± 0.07, $p > 0.05$; 12 h: $1.36 \pm 0. 15$, $p > 0.05$; 24 h: 1.65 ± 0.26, $p < 0.05$; 48 h: 5.78 ± 1.80, $p < 0.05$). In all experiments, the mRNA or protein levels were normalized to that of untreated controls. The results are shown as the means $\pm$ S.E. *n*, shown as *white numbers* in the *bars*, represents the number of independent culture preparations (*A*, *B*, and *D*) or the number of rats (*C*). *, $p < 0.05$; **, $p < 0.01$; ***, $p < 0.001$. *Ctrl*, control.

Where did the additional SST come from? In theory, it could either be from elevated SST expression and secretion in SST interneurons or ectopic expression of SST in neurons that normally do not express it. To address this question, we co-immunostained for SST, GABA, and MAP2 (neuronal marker) in DIV 12 hippocampal cultures. We found that under all of the conditions examined, including basal and activity elevation using 48 h of bicuculline, KA, or KCl treatments, SST expression was restricted to GABAergic interneurons (Fig. 2*A*). These results demonstrated that SST is expressed in DIV 12 neuronal cultures and that furthermore its cell type specificity is not altered following activity elevation.

To further examine whether this was also the case *in vivo*, we used the GAD67-GFP knock-in mice, which expressed GFP specifically in interneurons under the endogenous GAD67 promoter (35). We found a high level of co-localization between SST and GFP immunoreactivity in the CA1 region of the hippocampus (Fig. 2*B*), both under control conditions and 24 h following seizure induction through *in vivo* KA injection, further demonstrating that activity elevation does not affect the cell type specificity of SST expression.

Long Term SST Treatment Reduced the Density of Dendritic Spines and Excitatory Synapses, without Affecting Inhibitory Synapses—Having shown that SST expression and secretion are both induced by elevation in neuronal activity, we next

asked what could be its likely effect on neuronal morphology and function. The relatively long delay between the activity-induced increase in SST expression at 4 h (Fig. 1, *A* and *B*) and detectable increases in its secretion at 24 h (Fig. 1*D*) is temporally quite distinct from its previously described effects on neuronal excitability and synaptic transmission (14), which were fast acting and short-lived. Instead, they are more consistent with slow acting changes that occurred over an extended period, such as alterations in neuronal morphology. To assay the effects of SST on neuronal morphology, we applied 1 μM SST to DIV 14 and 15 hippocampal neuronal cultures to assay its effect on the dendritic spine density of pyramidal neurons 24 h later. We found that SST treatment significantly lowered spine density (Fig. 3, *A* and *B*), without affecting the average size of spines (Fig. 3*C*). Because dendritic spines are the morphological bases of excitatory synapses (39, 40), we next asked whether the reduction in spine density was due to lowered density of excitatory synapses.

Hippocampal neuronal cultures (DIV 10–12), treated with 1 μM SST for 24 h, were immunostained with vGluT1, a presynaptic marker of excitatory synapses, together with the active zone marker Bassoon. Only vGluT1 puncta co-localizing with Bassoon were considered synaptic. As compared with control untreated neurons, SST-treated pyramidal neurons had significantly reduced vGluT1 puncta density, measured as puncta
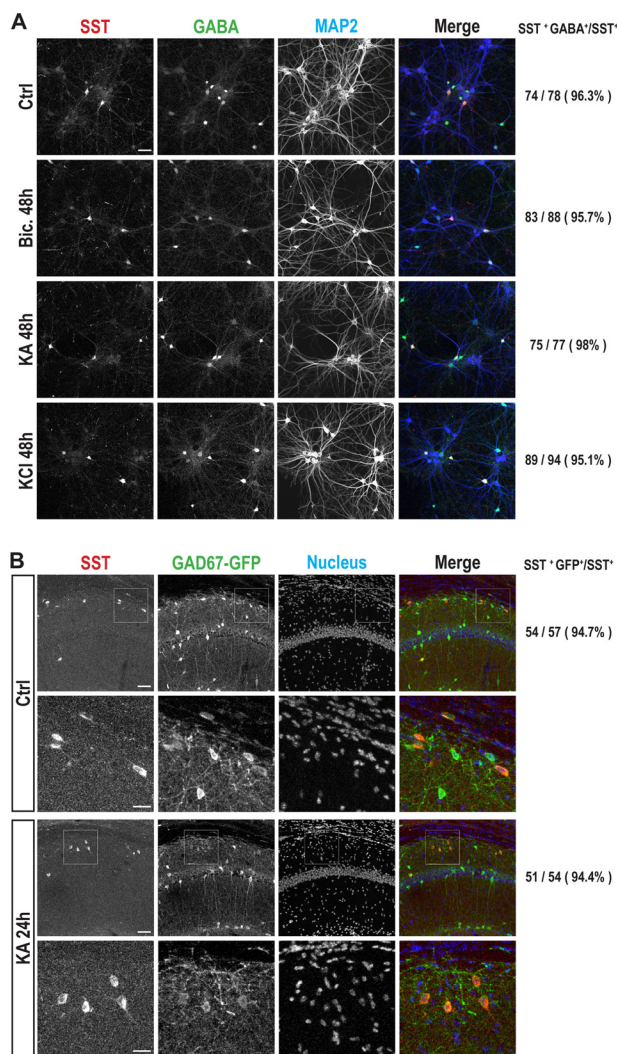
FIGURE 2. SST was specifically expressed in interneurons following activity elevation *in vitro* or *in vivo*. *A*, representative images of SST, GABA, and MAP2 immunostaining of DIV 12 primary hippocampal neurons, treatments as indicated. The *scale bar* is 50 μm. The number of neurons co-labeling with SST and GABA (SST$^+$ GABA$^+$), as a percentage of total SST immunopositive neurons (SST$^+$) is quantitated to the *right* of each example. *B*, representative images of the CA1 region of GAD67-GFP mice, untreated or 24 h following KA injection, channels as labeled. The *scale bar* is 50 μm for the *top row* of each condition and 20 μm for the zoomed images (*white boxes* of top rows) in the *bottom row* of each condition. The number of the neurons co-immunostaining with SST and GFP (SST$^+$ GFP$^+$), as a percentage of total SST immunopositive neurons (SST$^+$), is shown to the *right* of each example. *Ctrl*, control; *Bic.*, bicuculline.

number per unit length of dendrite (MAP2 immunostaining or GFP fluorescence) and no significant change in the integrated intensity of the average punctum (Fig. 3, *D* and *F*). Similarly, the density of postsynaptic AMPA subtype of glutamate receptors, as measured by surface GluR2 co-localizing with Bassoon, was also significantly reduced, whereas the integrated intensity of the average GluR2 punctum was not affected (Fig. 3, *E* and *G*). In contrast to the significant reduction in the density of glutamatergic synapses, the density of GABAergic inhibitory synapses, as measured using vGAT and GABA$_A$Rα1, was not affected by SST treatment (Fig. 3, *H–K*). Together, these results demonstrated that SST treatment specifically reduced the density of excitatory glutamatergic synapses, without affecting GABAergic synapses.

SST Treatment Reduced Excitatory Synaptic Transmission without Affecting Inhibition—To determine whether the observed effect of SST in reducing the density of dendritic spines (Fig. 3, *A* and *B*), and pre- and postsynaptic markers of excitatory synapses (Fig. 3, *D–G*), also lowered the number of functional excitatory synapses, we performed whole cell patch clamp recordings on SST-treated neurons. We found that 24 h of SST treatment significantly reduced the frequency of mEPSCs without affecting the amplitude of the average miniature event (Fig. 4, *A–D*). This reduction in mEPSC frequency is consistent with the observed reduction in the puncta density of vGluT1 and GluR2 (Fig. 3 *D–G*) and the lowered spine density (Fig. 3, *A* and *B*) providing further evidence that SST treatment significantly reduced the number of excitatory synapses, both morphologically and functionally. Consistent with the lack of changes in vGAT and GABA$_A$Rα1 (Fig. 3, *H–K*), we did not detect any changes in the amplitude or frequency of mIPSCs (Fig. 4, *E–H*).

The Effect of SST on Dendritic Spines and Excitatory Transmission Is Mediated by Postsynaptic SSTR4—Having shown that SST treatment significantly reduced dendritic spine density and the number of excitatory synapses on pyramidal neurons, we next asked through what mechanism are these effects mediated. SST receptors, of which there are five subtypes (SSTR1–5), are G protein-coupled receptors (41–43). Previous reports showed that SSTR4 is the main SST receptor subtype in CA1 and CA3 regions of the hippocampus (44, 45). Because the hippocampal neuronal cultures used in all our experiments were mixed hippocampal CA1/CA3 cultures with the dentate gyrus removed during dissection, we surmised that SSTR4 would be the predominant SST receptor subtype in our cultures. We thus designed a SSTR4-specific RNAi construct and showed that it effectively reduced the level of SSTR4 (Fig. 5*A*). Transfecting hippocampal pyramidal neurons with control or SSTR4 RNAi constructs, we showed that although reducing the endogenous level of SSTR4 by RNA interference did not affect spine density *per se*, it completely blocked the effect of SST treatment on reducing spine density (Fig. 5, *B* and *C*). SSTR4 RNAi did not affect the size of dendritic spines (Fig. 5*D*). Consistently, SSTR4 RNAi also completely blocked the effect of SST treatment on reducing mEPSC frequency, without affecting mEPSC amplitude or frequency by itself (Fig. 5, *E–H*). Together, these results suggest that the effects of SST in reducing the number of morphological and functional excitatory synapses are mediated through SSTR4 on pyramidal neurons.

DISCUSSION

In this study, we demonstrated a role for the activity-induced neuropeptide SST in regulating the morphology and function of excitatory synapses. Specifically, we showed that relatively long term treatment (24 h) of hippocampal neurons with SST significantly reduced the density of dendritic spines (Fig. 3, *A* and *B*), the density of pre- and postsynaptic markers of excitatory synapses (Fig. 3, *D–G*), and the frequency of mEPSCs (Fig. 4, *A–D*), without affecting inhibition (Figs. 3, *H–K*, and 4, *E–H*). We further showed that these effects of SST were mediated through the postsynaptic action of SSTR4 expressed on hippocampal pyramidal neurons (Fig. 5). Together, these results
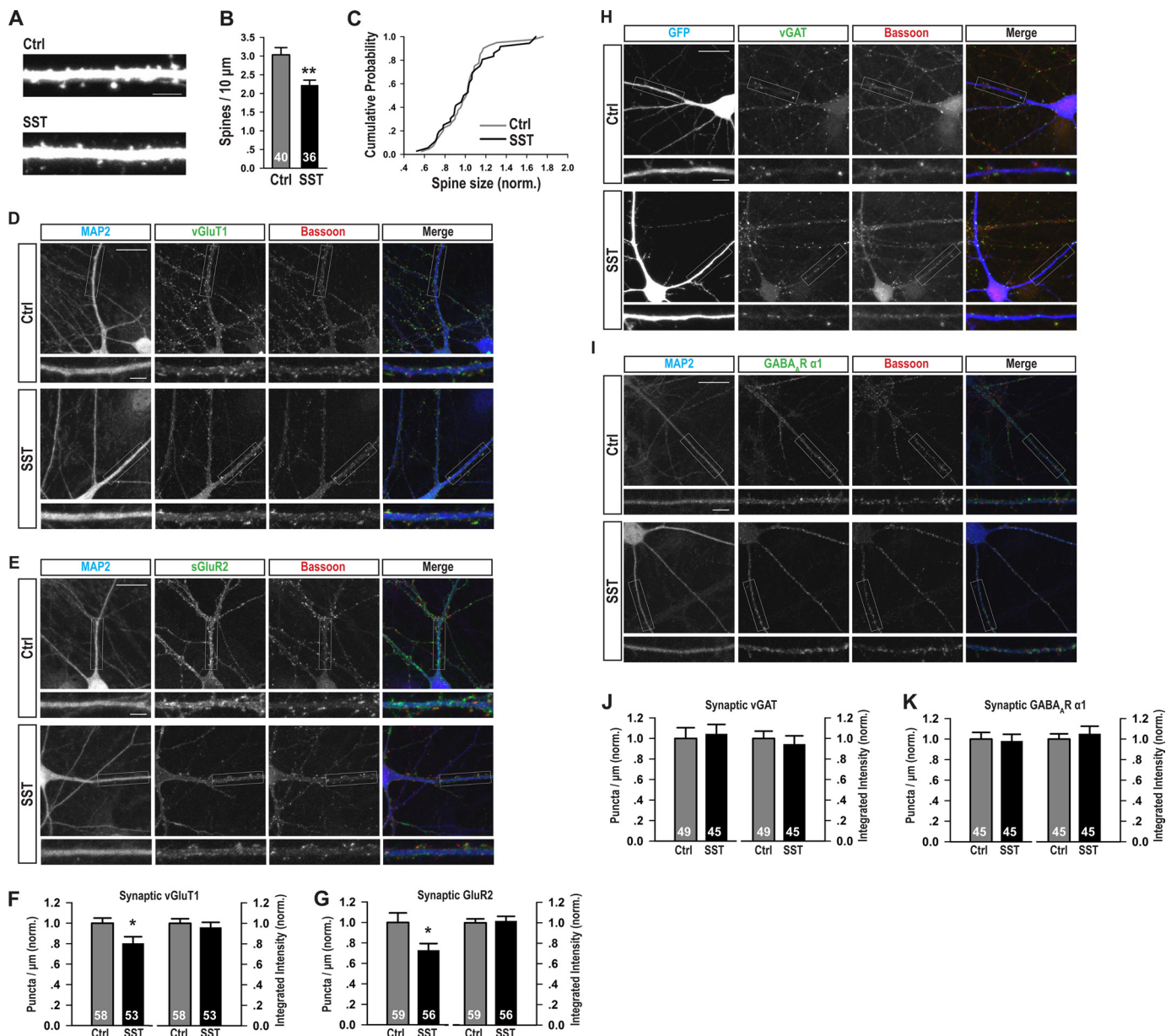
FIGURE 3. **SST treatment reduced the density of dendritic spine, as well as that of pre- and postsynaptic markers of excitatory synapses, without affecting inhibitory synapses.** *A*, representative images of the dendritic spines of control (*Ctrl*) neurons or those treated with SST. The *scale bar* is 5 μm. *B*, quantitation of dendritic spine density following SST treatment (control: 3.03 ± 0.19; SST: 2.22 ± 0.14, $p < 0.01$). *C*, SST treatment did not affect the size of dendritic spines: $p > 0.05$. *D*, *E*, *H*, and *I*, representative images of dendrites (labeled with MAP2 or GFP) immunostained with Bassoon and co-stained with vGluT1 (*D*), surface GluR2 (sGluR2, *E*), vGAT (*H*), or GABA$_A$Rα1 (*I*). The dendritic segment within each *white box* is shown as a zoomed image below. The *scale bar* is 20 μm for full frame images and 5 μm for the zoomed images. *F*, SST treatment reduced the density of synaptic vGluT1 (control: 1 ± 0.05; SST: 0.80 ± 0.07, $p < 0.05$), without affecting the integrated intensity of vGluT1 puncta (control: 1 ± 0.05; SST: 0.96 ± 0.05, $p > 0.05$). *G*, SST treatment reduced the density of synaptic GluR2 (control: 1 ± 0.09; SST: 0.73 ± 0.07, $p < 0.05$), without affecting the integrated intensity of synaptic GluR2 puncta (control: 1 ± 0.04; SST: 1.02 ± 0.05, $p > 0.05$). *J*, SST treatment did not affect the density (control: 1 ± 0.11; SST: 1.04 ± 0.09, $p > 0.05$) or integrated intensity (control: 1 ± 0.07; SST: 0.94 ± 0.08, $p > 0.05$) of synaptic vGAT puncta. *K*, the density (control: 1 ± 0.06; SST: 0.98 ± 0.07, $p > 0.05$) or integrated intensity (control: 1 ± 0.05; SST: 1.05 ± 0.08, $p > 0.05$) of synaptic GABA$_A$Rα1 was not affected by SST treatment. The results are shown as the means ± S.E. *n*, shown as *white numbers* in the *bars*, represents the number of neurons. *, $p < 0.05$; **, $p < 0.01$.

suggest a role for SST, secreted by the SST subtype of interneurons, in specifically down-regulating the number of excitatory synapses on pyramidal neurons following persistent and global elevation of neuronal activity. We propose that these morphological and functional changes induced by long term SST treatment likely contribute to its previously described anti-epileptic effect (31).

In contrast to the previously described effects of SST on potassium channel activity and excitatory synaptic transmis-

sion, which were fast acting and did not last long (26–28, 30), the effects we describe here take place over a more extended period. This is likely because morphological changes, especially ones involving the removal of existing synapses and spines, likely take place over the course of hours, rather than minutes (46, 47). This time course is consistent with the relatively slow induction in the gene expression and secretion of SST following global activity elevation (Fig. 1). The acute effect of SST on excitatory transmission was shown to act through activation of
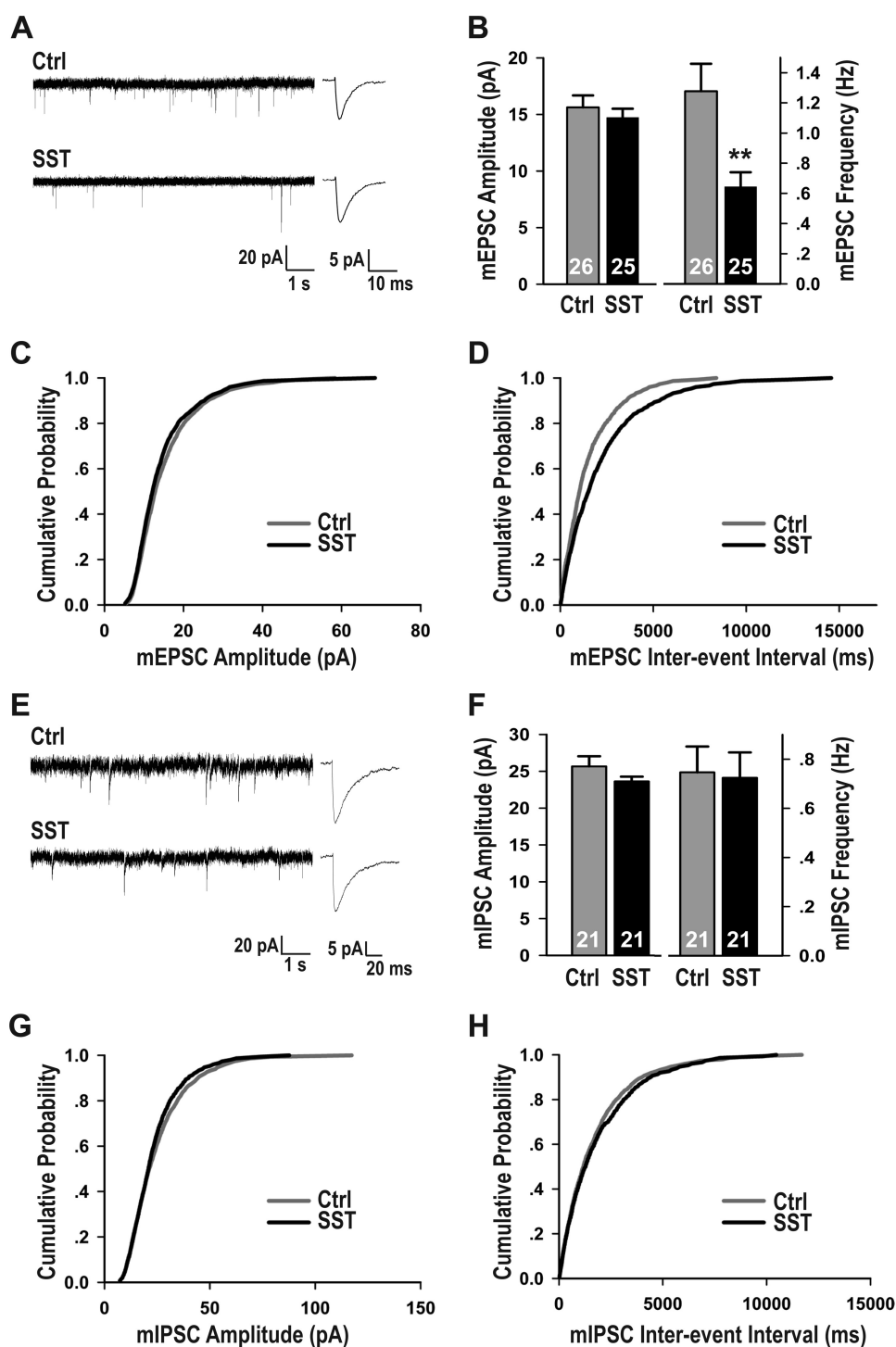
FIGURE 4. **SST treatment reduced the frequency of mEPSCs, without affecting mIPSCs.** *A*, representative mEPSC traces and average waveforms from Ctrl or SST-treated neurons. *B*, SST treatment did not affect the amplitude of mEPSCs (control: 15.62 ± 1.05 pA; SST: 14.73 ± 0.78 pA, $p > 0.05$) but significantly reduced their frequency (control: 1.28 ± 0.18 Hz; SST: 0.64 ± 0.10 Hz, $p < 0.01$). *C* and *D*, cumulative probability plot of mEPSC amplitudes ($p > 0.05$, *C*) and interevent intervals ($p < 0.01$, *D*). *E*, representative mIPSC traces and average waveforms from control and SST-treated neurons. *F*, SST treatment did not affect the amplitude (control: 25.67 ± 1.37 pA; SST: 23.62 ± 0.64 pA, $p > 0.05$) or frequency (control: 0.75 ± 0.11 Hz; SST: 0.72 ± 0.10 Hz, $p > 0.05$) of mIPSCs. *G* and *H*, cumulative distributions of mIPSC amplitudes ($p > 0.05$, *G*) or interevent intervals ($p > 0.05$, *H*). The results are shown as the means ± S.E. *n*, shown as *white numbers* in the *bars*, represents the number of neurons. **, $p < 0.01$.

its presynaptic receptor (29). In contrast, here we showed that the long term effect of SST on spine density was mediated by SSTR4 expressed on postsynaptic pyramidal neurons (Fig. 5). Thus, pre- and postsynaptic SST receptors seem to mediate distinct functions, with presynaptic receptors affecting transmitter release and postsynaptic SST receptors, such as SSTR4 expressed on pyramidal neurons, mediating the effect of SST in regulating the density of dendritic spines and excitatory synapses.

SST is thought to be an anti-epileptic agent based on following observations: 1) the expression and release of SST were
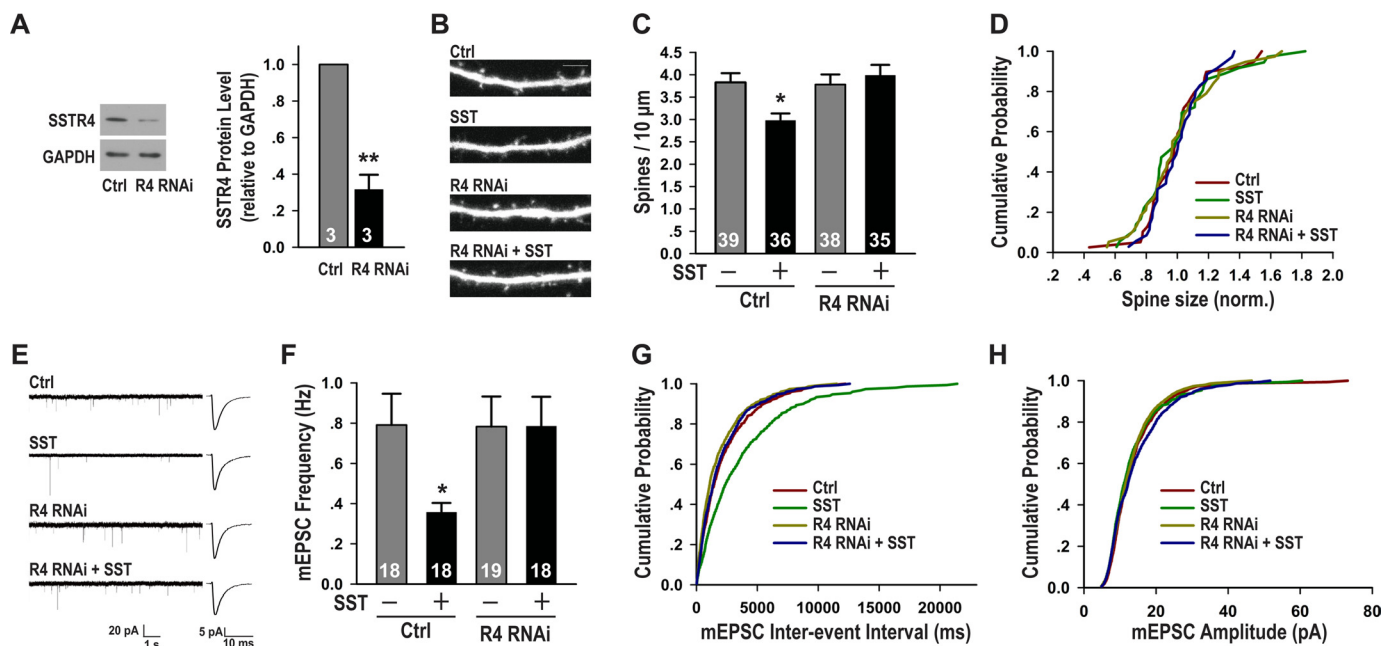
FIGURE 5. **The effects of SST on spines and mEPSCs were mediated by postsynaptic SSTR4.** *A*, the SSTR4 RNAi (*R4 RNAi*) was efficient in reducing the level of SSTR4 in hippocampal neurons (R4 RNAi: 0.32 ± 0.08, $p < 0.01$). *B*, representative images of dendritic spines, conditions as indicated. The *scale bar* is 5 μm. *C*, SSTR4 RNAi blocked SST-induced reduction in dendritic spine density (control: 3.83 ± 0.21; SST: 2.98 ± 0.16, $p < 0.05$ *versus* control; R4 RNAi: 3.78 ± 0.22, $p > 0.05$ *versus* control; R4 RNAi + SST: 3.99 ± 0.24, $p > 0.05$ *versus* R4 RNAi). *D*, none of the treatments affected the size of dendritic spines: $p > 0.05$ for all conditions. *E*, representative mEPSC traces and average waveforms, conditions as indicated. *F*, SSTR4 RNAi blocked the effect of SST on reducing mEPSC frequency (control: 0.79 ± 0.16 Hz; SST: 0.36 ± 0.05 Hz, $p < 0.05$ *versus* control; R4 RNAi: 0.78 ± 0.15 Hz, $p > 0.05$ *versus* control; R4 RNAi + SST: 0.79 ± 0.15 Hz, $p > 0.05$ *versus* R4 RNAi). *G*, cumulative distribution of interevent intervals (SST *versus* control: $p < 0.001$; R4 RNAi *versus* control: $p > 0.05$; R4 RNAi + SST *versus* R4 RNAi: $p > 0.05$). *H*, SSTR4 RNAi did not affect mEPSC amplitude in control or SST-treated conditions. $p > 0.05$ for all conditions. The results are shown as the means $\pm$ S.E. *n*, shown as *white numbers* in the *bars*, represents the number of neurons. *, $p < 0.05$; **, $p < 0.01$. *Ctrl*, control.

increased following seizures (14, 48–50); 2) SST application in hippocampal slices reduced neuronal firing and epileptiform activity (31); 3) injection of SST into the mouse brain reduced seizure, whereas application of anti-SST serum into mouse brain increased it (51); 4) SST knock-out mice have a shorter latency for stage 5 seizures (52), while SSTR4 knock-out mice displayed increased seizure sensitivity in both the pentylenetetrazole and kainic acid models (53). Our results, demonstrating a role for the interneuron-secreted neuropeptide SST in mediating activity-induced reduction in the density of dendritic spines and excitatory synapses through postsynaptic SSTR4 signaling, provide further insight into the molecular mechanism through which SST achieves its anti-epileptic effect.

We also note that in contrast to other activity-induced secreted factors previous identified, which have generally been shown to function in the same direction as neuronal activity to promote the development of neural circuits (7–9), activity-induced SST expression acts in the opposite direction to reduce the number of morphological and functional excitatory synapses on pyramidal neurons, thereby reducing overall activity in the neural network. This function of SST is consistent with it being an interneuron-secreted factor, because an important function of GABAergic interneurons is to dampen network activity, especially under conditions of overexcitation. Likely because of its role in reducing synapse number, SST gene expression and secretion are induced slowly and after a prolonged and global increase in activity. This slow induction allows it to reduce the risk of overexcitation without interfering with Hebbian plasticity mecha-

nisms such as long term potentiation. Given the prominence of SST-immunoreactive interneurons in the hippocampus and neocortex, representing approximately one-third of total interneurons (10–12), the effects of SST, such as its ability to reduce dendritic spine density following activity elevation, are likely to be physiologically important to the development and stability of neural circuits.

REFERENCES
1. Hofer, S. B., Mrsic-Flogel, T. D., Bonhoeffer, T., and Hübener, M. (2006) Lifelong learning. Ocular dominance plasticity in mouse visual cortex. *Curr. Opin. Neurobiol.* **16,** 451–459
2. Hua, J. Y., and Smith, S. J. (2004) Neural activity and the dynamics of central nervous system development. *Nat. Neurosci.* **7,** 327–332
3. Katz, L. C., and Shatz, C. J. (1996) Synaptic activity and the construction of cortical circuits. *Science* **274,** 1133–1138
4. Spitzer, N. C. (2006) Electrical activity in early neuronal development. *Nature* **444,** 707–712
5. Wong, R. O., and Ghosh, A. (2002) Activity-dependent regulation of dendritic growth and patterning. *Nat. Rev. Neurosci.* **3,** 803–812
6. Zhang, L. I., and Poo, M. M. (2001) Electrical activity and development of neural circuits. *Nat. Neurosci.* **4,** (suppl.) 1207–1214
7. Cohen, S., and Greenberg, M. E. (2008) Communication between the synapse and the nucleus in neuronal development, plasticity, and disease.

Annu. Rev. Cell Dev. Biol. **24,** 183–209

8. Flavell, S. W., and Greenberg, M. E. (2008) Signaling mechanisms linking neuronal activity to gene expression and plasticity of the nervous system. *Annu. Rev. Neurosci.* **31,** 563–590

9. Loebrich, S., and Nedivi, E. (2009) The function of activity-regulated genes in the nervous system. *Physiol. Rev.* **89,** 1079–1103

10. Jinno, S., and Kosaka, T. (2006) Cellular architecture of the mouse hippocampus. A quantitative aspect of chemically defined GABAergic neurons with stereology. *Neurosci. Res.* **56,** 229–245

11. Markram, H., Toledo-Rodriguez, M., Wang, Y., Gupta, A., Silberberg, G., and Wu, C. (2004) Interneurons of the neocortical inhibitory system. *Nat. Rev. Neurosci.* **5,** 793–807

12. Rudy, B., Fishell, G., Lee, S., and Hjerling-Leffler, J. (2011) Three groups of interneurons account for nearly 100% of neocortical GABAergic neurons. *Dev. Neurobiol.* **71,** 45–61

13. Vezzani, A., and Hoyer, D. (1999) Brain somatostatin. A candidate inhibitory role in seizures and epileptogenesis. *Eur. J. Neurosci.* **11,** 3767–3776

14. Tallent, M. K., and Qiu, C. (2008) Somatostatin. An endogenous antiepileptic. *Mol. Cell. Endocrinol.* **286,** 96–103

15. Brazeau, P., Vale, W., Burgus, R., Ling, N., Butcher, M., Rivier, J., and Guillemin, R. (1973) Hypothalamic polypeptide that inhibits the secretion of immunoreactive pituitary growth hormone. *Science* **179,** 77–79

16. Epelbaum, J. (1986) Somatostatin in the central nervous system. Physiology and pathological modifications. *Prog. Neurobiol.* **27,** 63–100

17. Rossignol, E. (2011) Genetics and function of neocortical GABAergic interneurons in neurodevelopmental disorders. *Neural Plast.* **2011,** 649325

18. Wonders, C. P., and Anderson, S. A. (2006) The origin and specification of cortical interneurons. *Nat. Rev. Neurosci.* **7,** 687–696

19. Karube, F., Kubota, Y., and Kawaguchi, Y. (2004) Axon branching and synaptic bouton phenotypes in GABAergic nonpyramidal cell subtypes. *J. Neurosci.* **24,** 2853–2865

20. Katona, I., Acsády, L., and Freund, T. F. (1999) Postsynaptic targets of somatostatin-immunoreactive interneurons in the rat hippocampus. *Neuroscience* **88,** 37–55

21. Murayama, M., Pérez-Garci, E., Nevian, T., Bock, T., Senn, W., and Larkum, M. E. (2009) Dendritic encoding of sensory stimuli controlled by deep cortical interneurons. *Nature* **457,** 1137–1141

22. Silberberg, G., and Markram, H. (2007) Disynaptic inhibition between neocortical pyramidal cells mediated by Martinotti cells. *Neuron* **53,** 735–746

23. Berger, T. K., Perin, R., Silberberg, G., and Markram, H. (2009) Frequency-dependent disynaptic inhibition in the pyramidal network. A ubiquitous pathway in the developing rat neocortex. *J. Physiol.* **587,** 5411–5425

24. Kapfer, C., Glickfeld, L. L., Atallah, B. V., and Scanziani, M. (2007) Supralinear increase of recurrent inhibition during sparse activity in the somatosensory cortex. *Nat. Neurosci.* **10,** 743–753

25. Ludwig, M., and Leng, G. (2006) Dendritic peptide release and peptide-dependent behaviours. *Nat. Rev. Neurosci.* **7,** 126–136

26. Moore, S. D., Madamba, S. G., Joëls, M., and Siggins, G. R. (1988) Somatostatin augments the M-current in hippocampal neurons. *Science* **239,** 278–280

27. Schweitzer, P., Madamba, S., and Siggins, G. R. (1990) Arachidonic acid metabolites as mediators of somatostatin-induced increase of neuronal M-current. *Nature* **346,** 464–467

28. Schweitzer, P., Madamba, S. G., and Siggins, G. R. (1998) Somatostatin increases a voltage-insensitive K+ conductance in rat CA1 hippocampal neurons. *J. Neurophysiol.* **79,** 1230–1238

29. Boehm, S., and Betz, H. (1997) Somatostatin inhibits excitatory transmission at rat hippocampal synapses via presynaptic receptors. *J. Neurosci.* **17,** 4066–4075

30. Tallent, M. K., and Siggins, G. R. (1997) Somatostatin depresses excitatory but not inhibitory neurotransmission in rat CA1 hippocampus. *J. Neurophysiol.* **78,** 3008–3018

31. Tallent, M. K., and Siggins, G. R. (1999) Somatostatin acts in CA1 and CA3 to reduce hippocampal epileptiform activity. *J. Neurophysiol.* **81,** 1626–1635

32. Peng, Y. R., Zeng, S. Y., Song, H. L., Li, M. Y., Yamada, M. K., and Yu, X.

(2010) Postsynaptic spiking homeostatically induces cell-autonomous regulation of inhibitory inputs via retrograde signaling. *J. Neurosci.* **30,** 16220–16231

33. Tan, Z. J., Peng, Y., Song, H. L., Zheng, J. J., and Yu, X. (2010) N-cadherin-dependent neuron-neuron interaction is required for the maintenance of activity-induced dendrite growth. *Proc. Natl. Acad. Sci. U.S.A.* **107,** 9873–9878

34. Shaner, N. C., Campbell, R. E., Steinbach, P. A., Giepmans, B. N., Palmer, A. E., and Tsien, R. Y. (2004) Improved monomeric red, orange and yellow fluorescent proteins derived from *Discosoma* sp. red fluorescent protein. *Nat. Biotechnol.* **22,** 1567–1572

35. Tamamaki, N., Yanagawa, Y., Tomioka, R., Miyazaki, J., Obata, K., and Kaneko, T. (2003) Green fluorescent protein expression and colocalization with calretinin, parvalbumin, and somatostatin in the GAD67-GFP knock-in mouse. *J. Comp. Neurol.* **467,** 60–79

36. Applied Biosystems (2001) *User Bulletin No. 2*, Rev B Applied Biosystems, Foster City, CA

37. Liu, N., He, S., and Yu, X. (2012) Early natural stimulation through environmental enrichment accelerates neuronal development in the mouse dentate gyrus. *PLoS One* **7,** e30803

38. He, S., Ma, J., Liu, N., and Yu, X. (2010) Early enriched environment promotes neonatal GABAergic neurotransmission and accelerates synapse maturation. *J. Neurosci.* **30,** 7910–7916

39. Alvarez, V. A., and Sabatini, B. L. (2007) Anatomical and physiological plasticity of dendritic spines. *Annu. Rev. Neurosci.* **30,** 79–97

40. Bourne, J. N., and Harris, K. M. (2008) Balancing structure and function at hippocampal dendritic spines. *Annu. Rev. Neurosci.* **31,** 47–67

41. Csaba, Z., and Dournaud, P. (2001) Cellular biology of somatostatin receptors. *Neuropeptides* **35,** 1–23

42. Viollet, C., Lepousez, G., Loudes, C., Videau, C., Simon, A., and Epelbaum, J. (2008) Somatostatinergic systems in brain. Networks and functions. *Mol. Cell. Endocrinol.* **286,** 75–87

43. Kumar, U., and Grant, M. (2010) Somatostatin and somatostatin receptors. *Results Probl. Cell Differ.* **50,** 137–184

44. Gastambide, F., Lepousez, G., Viollet, C., Loudes, C., Epelbaum, J., and Guillou, J. L. (2010) Cooperation between hippocampal somatostatin receptor subtypes 4 and 2. Functional relevance in interactive memory systems. *Hippocampus* **20,** 745–757

45. Schreff, M., Schulz, S., Händel, M., Keilhoff, G., Braun, H., Pereira, G., Klutzny, M., Schmidt, H., Wolf, G., and Höllt, V. (2000) Distribution, targeting, and internalization of the sst4 somatostatin receptor in rat brain. *J. Neurosci.* **20,** 3785–3797

46. Zuo, Y., Yang, G., Kwon, E., and Gan, W. B. (2005) Long-term sensory deprivation prevents dendritic spine loss in primary somatosensory cortex. *Nature* **436,** 261–265

47. Holtmaat, A. J., Trachtenberg, J. T., Wilbrecht, L., Shepherd, G. M., Zhang, X., Knott, G. W., and Svoboda, K. (2005) Transient and persistent dendritic spines in the neocortex *in vivo*. *Neuron* **45,** 279–291

48. Manfridi, A., Forloni, G. L., Vezzani, A., Fodritto, F., and De Simoni, M. G. (1991) Functional and histological consequences of quinolinic and kainic acid-induced seizures on hippocampal somatostatin neurons. *Neuroscience* **41,** 127–135

49. Hashimoto, T., and Obata, K. (1991) Induction of somatostatin by kainic acid in pyramidal and granule cells of the rat hippocampus. *Neurosci Res* **12,** 514–527

50. Wanscher, B., Kragh, J., Barry, D. I., Bolwig, T., and Zimmer, J. (1990) Increased somatostatin and enkephalin-like immunoreactivity in the rat hippocampus following hippocampal kindling. *Neurosci. Lett.* **118,** 33–36

51. Mazarati, A. M., and Telegdy, G. (1992) Effects of somatostatin and anti-somatostatin serum on picrotoxin-kindled seizures. *Neuropharmacology* **31,** 793–797

52. Buckmaster, P. S., Otero-Corchón, V., Rubinstein, M., and Low, M. J. (2002) Heightened seizure severity in somatostatin knockout mice. *Epilepsy Res.* **48,** 43–56

53. Qiu, C., Zeyda, T., Johnson, B., Hochgeschwender, U., de Lecea, L., and Tallent, M. K. (2008) Somatostatin receptor subtype 4 couples to the M-current to regulate seizures. *J. Neurosci.* **28,** 3567–3576